Information entropy and bound quantum states

Chandrachur Das
Department of Chemistry, B. C. College, Asansol 713 304, India

Kamal Bhattacharyya*
Department of Chemistry, University of Calcutta, 92 A.P.C. Road, Kolkata 700 009, India

(Received 3 October 2008; published 12 January 2009)

We explore a few advantages of studying the change in information entropy of a bound quantum state with energy. It is known that the property generally increases with the quantum number for stationary states, in spite of the concomitant gradual increase in the number of constraints for higher levels. A simple semiclassical proof of this observation is presented via the Wilson-Sommerfeld quantization scheme. In the small quantum number regime, we numerically demonstrate how far the semiclassical predictions are valid for a few systems, some of which are exactly solvable and some not so. Our findings appear to be significant in a number of ways. We observe that, for most problems, information entropy tends to a maximum as the quantum number tends to infinity. This sheds some light on the Bohr limit as a classical limit. Noting that the dependence of energy on the quantum number governs the rate of increase of information entropy with the degree of excitation, we extend our analysis to include the role of the kinetic energy. The endeavor yields a relation that possesses a universal character for any one-dimensional problem. Relevance of information entropy in studying the goodness of approximate stationary states obtained from finite-basis linear variational calculations is also delineated. Finally, we expound how this property behaves in situations where shape resonances show up. A typical variation is indeed observed in such cases when we proceed to detect Siegert states via the stabilization method.

DOI: 10.1103/PhysRevA.79.012107 PACS number(s): 03.65.Ge, 89.70.Cf

I. INTRODUCTION

The maximum entropy principle (MEP) [1,2] continues to be a subject of topical interest since inception. In simple terms, it states that the most likely distribution under a given set of constraints is the one that maximizes the information entropy. The MEP has provided initially a major impetus in the domain of statistical mechanics. However, it was soon felt that its numerical implementation demands careful consideration [3]. Later, practical applications have been made in such diverse fields as handling of divergent perturbation series [4,5], image reconstruction and spectral interpretation [6], polymer science [7], thermodynamics [8–10], etc.

Usually, in the MEP approach, one constructs a position probability density (PD) $P(x)$ with the assumption that the various power moments are available as input. The MEP prescription is to maximize the Boltzmann-Shannon information entropy (IE) I, defined by

$$I = -\int P(x)\ln P(x)dx, \tag{1}$$

subject to these moment constraints. The resultant $P(x)$ is believed to provide the least biased PD. Among other areas, extensive applications of the IE defined by Eq. (1) have been made in studies on orthogonal polynomials [11]. Its use in defining a thermodynamic length [12] seems also worth mentioning. In a purely quantum-mechanical context, attention has been focused on IE from several angles [13–19]. Primarily, the curiosity behind Eq. (1) grew out of the notions of IE in position and momentum spaces that led to entropic uncertainty relations [13]. The interest in this context still continues [14]. On the other hand, maximization of the IE in Eq. (1) with known values of the first few moments was pursued rather exhaustively by Plastino *et al.* [15] for a number of problems to find the ground quantum stationary states. We have later [16,17] found that, instead of supplying values for individual moments, one can profitably employ the principle with moment recursion relations as constraints. These recursion relations are obtainable by analyzing a given problem. Implementation of such a route yields nice results for both stationary ground quantum states [16,17] and classical chaotic states [16]. Dehesa *et al.* [18] pursued a neat WKB analysis to find the variation of IE with a quantum number for stationary states in x^{2M} potentials. Their study reveals an increase of I_n with n, except for confined systems. Later, the spectroscopic relevance of IE in the detection of avoided crossings has been highlighted [19], taking the explicit example of a H atom in the presence of an external perturbation.

The PD for a general excited quantum state Ψ_n is, however, difficult to construct via the MEP. One major trouble is to incorporate proper restrictions corresponding to the orthogonal and uncoupled nature of such a state with respect to *all* lower states. For a quantum system with the Hamiltonian H having exact eigenstates Ψ_m, this means one should satisfy $\langle\Psi_m|\Psi_n\rangle=\delta_{mn}$ and $\langle\Psi_m|H|\Psi_n\rangle=\delta_{mn}$ for all $m<n$. Additionally, one may recall that these constraints are to be used in conjunction with constraints imparted by moments, or moment recursion relations, in the course of maximizing I_n in Eq. (1) that refers now to the PD $|\Psi_n|^2$. Undoubtedly, things become quite messy then. On the contrary, a plain linear

*Author to whom correspondence should be addressed. pchemkb@yahoo.com

variational scheme [20] works very straightforwardly for excited states. So, this latter strategy provides a much better and sensible alternative. Therefore the relevance of the MEP to excited stationary quantum states should be sought elsewhere.

An alternative idea [18] in the present context is to study the dependence of IE on the quantum number n, instead of maximizing the MEP functional with an appropriate number of constraints. Apparently, one expects I_n to decrease with n because of the increasing number of nodes in states Ψ_n that raises the number of constraints. The uncoupling mentioned above adds to these restraints. But, this decrease is never observed [18]. Indeed, there exists a competing factor for systems that are *not* confined. As n increases, Ψ_n becomes more delocalized, leading to an enhancement of the IE, and this dominates the overall behavior. Such an observation seems to possess an immediate implication. The limit $n \to \infty$ is the Bohr (classical) limit. Therefore the variation of I_n as $n \to \infty$ may offer us a clue to appreciate this classical limit too, thus expanding the horizon of applicability of the MEP. Another domain where the variation of I_n vs n could be important is concerned with *approximate* stationary states. However, no such study is available. The primary motivation behind these studies is that most quantum-mechanical problems are not exactly solvable and therefore one has to deal with approximate states only. Besides, it is of interest to test the adequacy of semiclassical predictions for I_n in cases of near-exact stationary quantum states, and particularly in the small-n regime. Further, since the IE is a measure of the delocalization of the PD, and we know that localization increases the kinetic energy of a state, it is tempting to seek a relation between the IE and the average kinetic energy. We may emphasize at this point that, while the relation between kinetic energy and Boltzmann-Shannon IE that will emerge from our analysis is indirect, such a relation exists very directly in the Fisher information (FI) measure [21–24]. Therefore a link between the two information measures may be found. Noting further that a variety of routes are available to construct an approximate stationary state, we may also explore whether IE plays any role in estimating the goodness of such a state. Finally, certain Hamiltonians do not support bound states. But, in the presence of small tunneling terms, one can get long-lived quasibound states. The real energy parts of these states are obtainable from real square-integrable functions. There are various ways of achieving this end [25–27]. It seems worthwhile to inspect whether the IE plays any role during studies on such bound states.

In view of the above discussion, the present communication is aimed at the following studies. First, we arrive at a few semiclassical results on the basis of the Wilson-Sommerfeld (WS) rule [28]. This route is easier and leads to certain simple relations between the IE and the quantum number. Second, we test the adequacy of all the results in the small-n regime with exact or near-exact PD. Our approach yields certain useful bounds to the IE as well. Third, the WS route yields nicely a link between IE and the average kinetic energy. We notice that the relationship finds very satisfactory calculational support. It also reveals a link between IE and the FI. Fourth, we concentrate on linear variations and employ the IE to assess the goodness of states. This endeavor, as we shall see, is rewarding too. It is quite comparable with standard measures, but is otherwise simple. Our final objective is to analyze how the IE behaves during the detection of resonant states via the stabilization method. It will be seen that the IE offers a few definitive indications about the existence of such states.

To proceed, we concentrate on square-integrable, time-independent quantum states, and take $\hbar = 1$ and $m = \frac{1}{2}$ throughout the study. Demonstrative pilot calculations involve problems in one dimension. These include the particle in a box, the harmonic and various anharmonic oscillators for which exact or near-exact PD are obtainable. Both stationary and Siegert states are considered in the present study. For the latter, bound wave functions are taken to extract the real energy parts only. Needless to mention, the calculations presented here should apply to problems in higher dimensions without much trouble. Thus our conclusions are quite general in character. All the chosen potentials are real, and so we employ real Ψ_n wherever necessary.

II. A SEMICLASSICAL ANALYSIS

Most quantum systems are not exactly solvable. So, one can hope to extract some general results in the current context only by having recourse to some semiclassical (SC) scheme [18]. We choose here the WS formalism for convenience.

The WS scheme starts with the quantization formula

$$\oint p dx = 2n\pi, \tag{2}$$

where $p \equiv p(x)$ is the momentum given by

$$p = [E - V(x)]^{1/2}. \tag{3}$$

If the classical turning points at the left and right sides are denoted respectively, by X_L and X_R, we can express Eq. (2) as

$$\int_{X_L}^{X_R} p dx = n\pi. \tag{4}$$

Now, we stick to the traditional wisdom of viewing probability as inversely proportional to speed and write

$$P(x) = N/p, \tag{5}$$

where N is the normalization constant and the PD so defined in Eq. (5) extends over the range $X_L \leqslant x \leqslant X_R$. We thus have

$$\int_{X_L}^{X_R} P(x) dx = 1 \tag{6}$$

and

$$\int_{X_L}^{X_R} [E - V(x)]^{1/2} dx = n\pi \tag{7}$$

that follows from Eq. (4). Differentiating Eq. (7) with respect to n via the Liebniz rule [29], we find that

$$\frac{dE}{dn}\int_{X_L}^{X_R}[E-V(x)]^{-1/2}dx=2\pi. \tag{8}$$

Making use of Eqs. (5) and (6), this result may be recast to obtain the following expression for N:

$$N=\frac{1}{2\pi}(dE/dn). \tag{9}$$

On the other hand, one may rewrite Eq. (7) in the form

$$N\langle P^{-2}\rangle=n\pi, \tag{10}$$

where the averaging in Eq. (10) involves the PD $P(x)$ itself. We need to now make one further approximation, viz. $\langle y^m\rangle=\langle y\rangle^m$, $\langle y\rangle\neq 0$, that is prevalent in the semiclassical domain. The basis behind the choice is that quantum fluctuations are expected to vanish in the semiclassical limit. Specifically for stationary quantum states, semiclassical results are known to agree with near-exact ones in the large quantum number limit, i.e., when $n\to\infty$. So, such an approximation is often used [30] to advantage in the domain concerned. Then, of course, from Eq. (10), we recover that

$$\langle P\rangle=(N/n\pi)^{1/2}. \tag{11}$$

With this approximation, we now proceed to Eq. (1) that may be rewritten as

$$I_n=-\langle \ln P_n\rangle. \tag{12}$$

The standard arithmetic-geometric mean inequality [29] may here be invoked profitably to obtain further

$$I_n\geqslant -\ln\langle P_n\rangle=J_n. \tag{13}$$

Using Eq. (11) at the right side of Eq. (13) in conjunction with Eq. (9), we next find that

$$J_n(\mathrm{SC})=-\ln(N/n\pi)^{1/2}=-\ln\left(\frac{dE}{dn}\Big/\,2n\pi^2\right)^{1/2}, \tag{14}$$

where we have explicitly taken care of the fact that Eq. (14) is a SC result for J_n. We now realize that the n dependence of J_n (SC) is crucially governed by the (dE/dn) term. Let us choose

$$dE/dn=\alpha n^{\beta}. \tag{15}$$

The following form for J_n is then obtained:

$$J_n(\mathrm{SC})=\ln(\pi\sqrt{2})-\frac{1}{2}\ln(\alpha\beta)-\frac{1}{2}(\beta-2)\ln n. \tag{16}$$

Finally, Eqs. (12) and (13) are exact relations. But, Eq. (16) involves a number of approximations and therefore it is not clear whether an inequality of the form $I_n\geqslant J_n$ (SC) will also be satisfied. However, one can safely write for the IE, in the absence of more rigorous results, that

$$I_n\approx\ln(\pi\sqrt{2})-\frac{1}{2}\ln(\alpha\beta)-\frac{1}{2}(\beta-2)\ln n. \tag{17}$$

Certainly Eq. (17) is an approximate result. Yet, we shall see that the chief conclusions based on it remain true even in the proper quantum domain. The only exception is the $n=0$ state for which Eq. (17) does not work. This is a reflection of the notion that the ground state is the *most* nonclassical state. Otherwise, Eq. (17) is a useful result. In particular, the following observations are worth noting in the context concerned:

(i) For the particle-in-a-box and related confined systems, e.g., its SUSY partner potential [31], we have the maximum possible value of $\beta=2$. Therefore I_n does not change with n at all. Specifically for the box, we have $E_n=(\pi/L)^2n^2$. Employing this expression in Eq. (17), one gets

$$I_n\approx\ln L. \tag{18}$$

This logarithmic length dependence changes over to the volume dependence in three dimensions and reminds us of a similar kind of dependence of thermodynamic entropy on the volume of an ideal gas.

(ii) The n independence of I_n for confined systems signifies that the decrease in I_n due to increasing nodal constraints (in Ψ_n) with n is *exactly* balanced by the concomitant tendency of $P_n=(\Psi_n)^2$ to gradually occupy the whole of the available space L. The implication is clear. One should then expect I_n to increase with n for any problem where the distance between the classical turning points widens with excitation.

(iii) For any other one-dimensional system, $\beta<2$. Therefore Eq. (17) tells us that I_n would increase with n. This at once strengthens our inference made just above. The slow but sure enhancement of IE towards infinity has also a direct bearing on the "classicality" of a state, because the $n\to\infty$ limit is the Bohr classical limit.

(iv) Particularly for the harmonic oscillator problem with force constant $K=2$, we have $E_n=2n$. Thus from Eq. (17) we obtain in this case

$$I_n\approx\ln\pi+\frac{1}{2}\ln n. \tag{19}$$

The slope in Eq. (19) matches exactly with the WKB prediction [18]. Its usefulness will concern us later.

(v) As a final point, we note from Eq. (17) that the slope of I_n vs $\ln n$ curve depends on a simple function of β [see Eq. (29) later]. In practical situations, we shall demonstrate the worth of this relation too.

III. SOME RESULTS

In this section, we shall systematically proceed to check how far the IE obeys the SC predictions in cases where exact or near-exact results can be obtained. Therefore we first focus attention on the particle-in-a-box problem and next consider the harmonic oscillator case. In the latter situation, we also explore the possibility of a bound to IE and the exact SC limit. Finally, we deal with quite a few nontrivial anharmonic oscillators.

A. Exact result for the box problem

As an example of a confined system, we choose the particle-in-a-box problem. For such a system in $(0,L)$, we have the PD

$$P_n = \frac{2}{L}(\sin n\pi x/L)^2. \tag{20}$$

Using this, we find

$$\begin{aligned} I_n &= -\langle \ln P_n \rangle \\ &= -\ln 2 + \ln L - \frac{2}{\pi}\int_0^\pi \sin^2 x \ln(\sin^2 x)dx \\ &= -0.3069 + \ln L \end{aligned} \tag{21}$$

that shows a close correspondence with the approximate result Eq. (18) except for the extra constant term in Eq. (21). However, the comment below Eq. (18) applies here too. If we compute the entropy change, the constant term will vanish, leaving behind only the logarithmic dependence on volume in three dimensions. It is also transparent from Eq. (21) that no n dependence of IE exists for this problem. Therefore our SC conclusion (ii) of Sec. II is retained.

B. Exact and approximate estimates for the harmonic oscillator case

It is tempting to check whether a few other WS predictions essentially hold in other bound-state problems as well. To this end, we first consider the harmonic oscillator case. The oscillator is defined by the Hamiltonian

$$H = -d^2/dx^2 + x^2. \tag{22}$$

The PD is known exactly for this problem and is given by

$$\Psi_n^2(x) = P_n(x) = \frac{1}{2^n n!\sqrt{\pi}} H^2(n,x)\exp[-x^2]. \tag{23}$$

The IE for some nth state is then computed via the relation $I_n = -\langle \ln P_n \rangle$ and the values for a number of states are given in Table I. Unlike the SC case, we also have here an exact bound to I_n as

$$I_n \geqslant -\ln\langle P_n \rangle. \tag{24}$$

These estimates are presented in Table I as well. As a third measure, one can approximate the Hermite polynomials $H(n,x)$ for large n, average out small oscillations, and obtain for $P_n(x)$ the SC form

$$P_n(x) = \frac{1}{\pi\sqrt{2n+1-x^2}} \tag{25}$$

to calculate $I_n = -\langle \ln P_n \rangle$ over the interval $-(2n+1)^{1/2} \leqslant x \leqslant (2n+1)^{1/2}$. These values are expected to furnish lesser percentage errors as n increases and can easily be computed even for quite large n. The table also contains such SC estimates at the last entry. Notably, in each case, we simultaneously estimated $\langle x^2 \rangle$ that has an exact value of $n+\frac{1}{2}$. This provides a good check for the accuracy of the numerical integrations involved.

In Fig. 1, we plot the various estimates of IE against n to substantiate the worth of the endeavor. The bounding nature of curve 2 is satisfying. One also sees that the SC results (curve 3) correspond to exact ones (curve 1) more closely as n increases. Moreover, some sort of a logarithmic dependence of I_n on n is apparent. An approximate SC analysis led us to Eq. (19). So, we next proceed to explore how far Eq. (19) is obeyed with exact quantum-mechanical and SC results. A least square fit of the last six SC data of Table I yields

$$I_n = 0.808\ 73 + 0.498\ 25 \ln n. \tag{26}$$

This compares nicely with Eq. (19), keeping in mind the rather rough character of Eq. (19). The slope is nearly ex-

TABLE I. Exact and approximate values of I_n for various states of the harmonic oscillator. The second column shows exact results, the fourth one gives lower bounds [see Eq. (24)]. The last column displays SC estimates on the basis of Eq. (25).

n	I_n	n	I_n	n	I_n
0	1.072	0	0.919	0	0.452
1	1.343	1	1.207	5	1.651
2	1.499	2	1.364	6	1.734
3	1.610	3	1.474	8	1.868
4	1.697	4	1.558	10	1.974
5	1.768	5	1.626	12	2.061
6	1.829	6	1.684	15	2.169
7	1.882	7	1.734	16	2.200
8	1.929	8	1.778	20	2.308
9	1.972	9	1.818	25	2.417
10	2.010	10	1.854	30	2.507
12	2.078	12	1.916	40	2.649
14	2.137	14	1.970	50	2.759
16	2.189	16	2.018	60	2.849
18	2.235	18	2.060	70	2.926
20	2.277	20	2.098	80	2.992
22	2.315	22	2.132	90	3.051
24	2.350	24	2.164	100	3.103
26	2.383	26	2.194	110	3.151
28	2.413	28	2.221	120	3.194
30	2.442	30	2.246	130	3.234

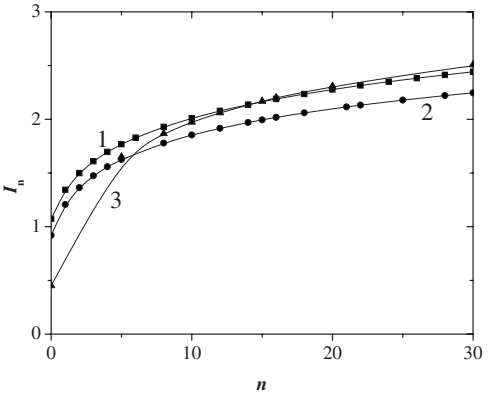

FIG. 1. Variation of I_n vs n is shown for the harmonic oscillator case. Curves 1, 2, and 3 refer, respectively, to the exact, lower bound, and SC results.

TABLE II. Near-exact values of I_n for various states of the quartic, sextic, and octic anharmonic oscillators, corresponding to $M=2$, 3, and 4 in Eq. (28).

n	I_n $(M=2)$	I_n $(M=3)$	I_n $(M=4)$
0	0.908	0.824	0.769
2	1.140	0.970	0.869
4	1.264	1.058	0.935
6	1.348	1.118	0.982
8	1.411	1.165	1.018
10	1.463	1.202	1.047
12	1.507	1.234	1.072
14	1.544	1.261	1.093
16	1.578	1.285	1.112
18	1.607	1.307	1.129
20	1.634	1.327	1.145
22	1.659	1.345	1.159
24	1.682	1.361	1.172
26	1.703	1.377	1.184
28	1.722	1.391	1.195
30	1.741	1.405	1.206

actly reproduced. Only, the constant factor is somewhat off from the earlier estimate. Interestingly, the exact estimates show a nice trend of approaching Eq. (26). A similar fitting with six *exact* data taken from Table I for n ranging from 10 to 20 and from 20 to 30 leads, respectively, to the following equations:

$$I_n = 1.121\ 16 + 0.385\ 39 \ln n,$$

$$I_n = 1.057\ 88 + 0.406\ 76 \ln n. \tag{27}$$

For still larger n, one expects that a variation like Eq. (26) will be gradually approached. It is reasonable to guess at this stage that, whatever may be the constant factor, the slope of the I_n vs $\ln n$ curve should finally settle at 0.5 [18]. And, this should be true for both exact and the SC estimates. We shall later see the adequacy of this presumption.

C. Behavior of anharmonic oscillators

Turning attention to a few nontrivial cases where exact PD is unknown for any state, let us choose the oscillators

$$H = -d^2/dx^2 + x^{2M}, \quad M = 2,3,4. \tag{28}$$

In such cases, we calculate the IE for specific states by first finding near-exact solutions for the PD with the help of a coupled linear-nonlinear variational strategy [32] that has earlier been found useful to tackle a variety of problems. Table II summarizes our results for the even parity states up to $n=30$. This would suffice for our present purpose. A plot of these results in Fig. 2 is again suggestive of a logarithmic rise with n of I_n. This is in conformity with our SC prediction in Eq. (17). One thus finds how useful it is to follow a WS type SC scheme.

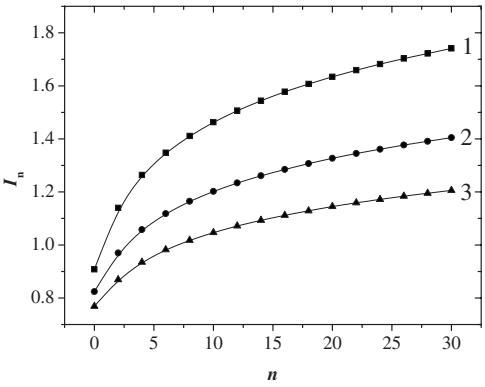

FIG. 2. Plots of I_n vs n for the systems defined by Eq. (28) with near-exact estimates. A slower rate of increase is evident for larger M.

Figure 3 shows the variation of I_n with $\ln n$ for all the oscillators under study in Eq. (28) including the $M=1$ case. Two important observations here are the following: As M increases, the rise of I_n becomes gradually less pronounced. One additionally observes that, although a strict linearity is not maintained, the slope of each such curve gently rises with rise of n. The message is transparent. If we concentrate on Eq. (17), the implication is the gradual rise of β with M. Coupled with our second observation, the expectation is that the slope of the curve of I_n vs $\ln n$ would approach the value $(2-\beta)/2$ as $n \to \infty$. It is easy to work out the value of β for various x^{2M} oscillators. This reads as

$$\beta = 2 \Big/ \left(1 + \frac{1}{M}\right). \tag{29}$$

From Eq. (29), one can get the correct slopes predicted by Eq. (17) in each case of M (1–4). This agrees with the WKB estimate (see Eq. (21) of Ref. [18]). Writing now

$$I_n = c + d \ln n, \tag{30}$$

one can estimate d via the relation

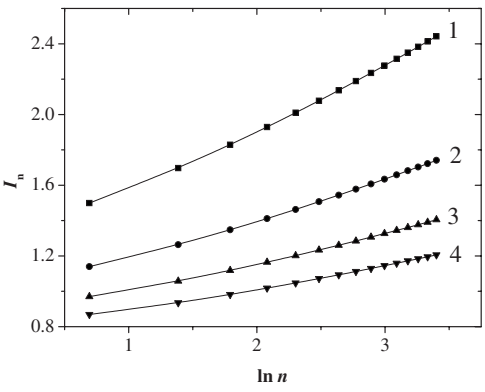

FIG. 3. Curves showing the dependence of I_n vs $\ln n$ with exact or near-exact estimates. Lines 1–4 correspond to the same values of M in Eq. (28).

TABLE III. Variation in values for the slope d in Eq. (30) in accordance with Eq. (31) for the set of oscillators given by Eq. (28) starting from $M=1$ up to $N=4$.

$n+2$	Quadratic	Quartic	Sextic	Octic
12	0.3731	0.2388	0.1737	0.1354
14	0.3811	0.2443	0.1779	0.1390
16	0.3874	0.2490	0.1815	0.1418
18	0.3927	0.2522	0.1844	0.1443
20	0.3970	0.2561	0.1868	0.1464
22	0.4009	0.2586	0.1890	0.1479
24	0.4042	0.2609	0.1908	0.1495
26	0.4072	0.2626	0.1927	0.1509
28	0.4097	0.2641	0.1932	0.1525
30	0.4122	0.2683	0.1964	0.1534
…	…	…	…	…
[1/1]	0.4510	0.3000	0.2210	0.1729
Exact	(1/2)	(1/3)	(1/4)	(1/5)

$$d \equiv d_{n+2} = \frac{I_{n+2} - I_n}{\ln(1 + 2/n)}. \tag{31}$$

Using near-exact results presented in Tables I and II, we compute Eq. (31) and display the data for various cases in Table III. A steady, monotonic approach to some limiting value in each case is seen clearly. We subsequently construct a [1/1] Padé approximant to accelerate the convergence. These values are shown in the penultimate row. The last row shows exact results in parentheses. By these exact results, we mean that $d=(2-\beta)/2$ in accordance with Eq. (17) where β is fixed by Eq. (29). We happily note the approach of d in Eq. (31), using exact estimates of IE, towards the values predicted by the SC route, though we have gone up to a maximum of $n=30$. Once more, the moral is that one can confide on the major parts of the SC analysis.

IV. FURTHER OBSERVATIONS

We now present four more important aspects of the preceding analysis. One is an extension of the SC result (14) that avoids the use of Eq. (15). This is particularly vital for practical problems where the potential does not have a simple power-law form, and hence either β is not easy to obtain, or the energy is not a simple function of n. Additionally, our approach will directly link the average kinetic energy of a state with its IE. Since it is known that the FI is straightforwardly related with the average kinetic energy [21,24], we next seek the kinship of the two information measures. Another point of interest lies in linear variational calculations that are routinely done in most quantum chemistry applications. Here, it is a standard wisdom that diagonalization of a $K\times K$ Hamiltonian matrix generates best the ground state. For excited states, eigenvectors and eigenvalues are always obtained with gradually rising errors. Still, one expects that a reasonable quality is maintained for roughly the first $K/2$ states. Normally, this is experienced by increasing the number K of the given basis set and comparing the energies against the earlier ones. An alternative is to check the computed data against known accurate estimates. Another option is to verify certain consistency requirements involving properties like, e.g., the virial theorem. Otherwise, one is forced to increase K to proceed towards a tedious job of estimating energies. We shall see the advantage of using IE in such cases. Indeed, I_n offers a simple kind of self-check that needs neither better available data set nor any routine increase of K. Finally, we explore the character of IE in calculations of Siegert states via the stabilization method, where a coupled linear-nonlinear variational scheme is employed and from the variations of energies as functions of the nonlinear parameter a quasibound state is detected (see, e.g., Ref. [27] for details).

A. Role of the kinetic energy

An increase of the IE is associated with spatial delocalization. On the other hand, the average kinetic energy of a state increases with confinement. Therefore it is natural to expect a link between I_n and $\langle T\rangle_n$ for a state n. The SC development on the basis of the WS scheme sketched in Sec. II yields nicely such a relation. To this end, we rewrite Eq. (7) as

$$\frac{1}{N}\langle p^2\rangle = n\pi, \tag{32}$$

with the help of Eqs. (5) and (6). Let us note that Eq. (10) is another useful way of writing Eq. (7) that has already been used. Symbolizing the kinetic energy by T, we now rearrange Eq. (32) as

$$\langle T\rangle_n = n\pi N. \tag{33}$$

In conjunction with Eq. (9), this leads to

$$dE/dn = 2\langle T\rangle_n/n. \tag{34}$$

Thus we can reframe Eq. (14) in the form

$$J_n(\mathrm{SC}) = -\ln(\langle T\rangle_n/n^2\pi^2)^{1/2} \tag{35}$$

that bypasses the (dE/dn) term. Consequently, Eq. (17) may now be replaced by

$$I_n \approx \ln \pi + \frac{1}{2}\ln\left(\frac{n^2}{\langle T\rangle_n}\right). \tag{36}$$

In view of such a relation, it is expected that a plot of the IE vs $\ln(n^2/\langle T\rangle_n)$ would give a straight line with a *fixed* slope of $\frac{1}{2}$ for *any* problem, as opposed to the β-dependent slope in Eq. (17). However, the catch is that Eq. (36) is strictly valid only in the $n\to\infty$ limit. But, as we saw earlier, such SC relations are approximately obeyed even in the small-n regime. For Eq. (36) to work, we only require to start from some n value that satisfies the inequality $n^2>\langle T\rangle_n$. Then, one would notice particularly that the predicted linearity is not lost, though calculated slopes and intercepts do not match closely with Eq. (36). Figure 4 displays two sample cases of pure sextic and octic oscillators. The plots are quite linear, as is evident from observed correlation coefficient values

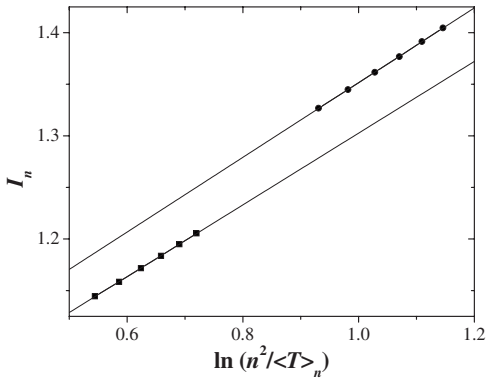

FIG. 4. Verification of the linearity predicted by Eq. (36) is displayed. The lower and upper lines refer, respectively, to $M=4$ and 3 in Eq. (28). In each case, we consider even n values ranging from 20 to 30.

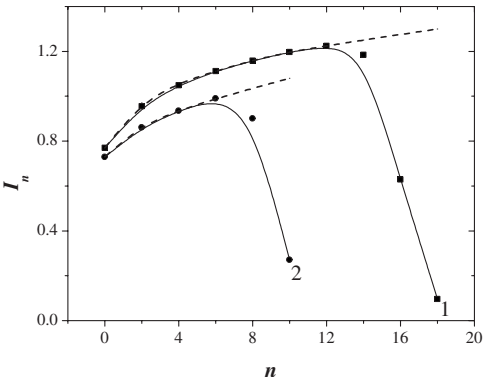

FIG. 5. Checking the adequacy of finite-basis calculations from plots of I_n vs n. Curves 1 and 2 show, respectively, a ten-basis calculation for the x^2+x^6 oscillator and a six-basis calculation for the x^2+x^8 oscillator, indicating certain states that are grossly in error.

$\geqslant 0.999$. A least squares fit with $\ln(n^2/\langle T\rangle_n)$ as x and I_n as y yields, respectively, for $M=4$ and 3

$$y = 0.954\,85 + 0.347\,78x,$$

$$y = 0.989\,42 + 0.362\,19x. \tag{37}$$

The kinship with Eq. (36) is very apparent from results (37). The slopes are expected to gradually rise to the theoretical value of 0.5 as we go for larger n values. Also, here we see straight from Eq. (36) that the box-type confined systems cannot show any variation of I_n with n because $\langle T\rangle_n$ itself increases as n^2.

B. Link with the Fisher measure for bound stationary states

We indicated earlier that the FI essentially uses the average kinetic energy as its measure. It is given by [21]

$$I_f = \int \frac{1}{P(x)}\left(\frac{dP(x)}{dx}\right)^2 dx \tag{38}$$

that is to be minimized. This definition should be contrasted with Eq. (1). Let us note that Eq. (38) has been employed in a wide variety of contexts too. For example, it worked as a part of a penalty function in arriving at the Schrödinger equation [21]. Its use as an entropy function yields the usual structure of thermodynamics [22]. Applied to central potentials, the measure leads to interesting inequalities between position and momentum space properties reflecting the uncertainty principle [23]. A recent, detailed exposition by Nalewajski [24] revealed the role of FI in various quantum-chemical problems, including certain aspects of the density-functional theory. In the present context, we take real Hamiltonians for which the eigenfunctions can always be chosen as real. Hence putting $P(x) \equiv P_n(x) = \Psi_n^2$, we obtain from Eq. (38)

$$I_f(n) = 4\int \left(\frac{d\Psi_n}{dx}\right)^2 dx = \frac{4}{\hbar^2}\langle p^2\rangle_n = \frac{8m}{\hbar^2}\langle T\rangle_n. \tag{39}$$

The proportionality of I_f with kinetic energy follows for complex functions as well [24]. However, we may now utilize Eq. (39) to rewrite Eq. (36) as

$$I_n \approx A + \ln n - \frac{1}{2}\ln I_f(n) \tag{40}$$

that shows a clear link between Shannon and Fisher information measures for energy eigenstates. Needless to mention, we have put all the constant terms (and m) in A in Eq. (40). This result has a nice physical appeal. An increase in FI is seen to reduce IE. Keeping it in mind that FI is minimized while IE is maximized, one can immediately seek an explanation of this fact. For real wave functions as chosen above, one obtains $\langle p\rangle_n = 0$. Thus from Eq. (39), we notice that minimization of FI is equivalent to minimizing the momentum uncertainty for a given state. This naturally maximizes the positional uncertainty, which means maximizing the delocalization in space and hence maximization of IE. We therefore recognize transparently that the two information measures basically work in complementary spaces. This is precisely the reason why one of them is maximized while the other is minimized.

C. Finite-basis linear variational calculations for bound states

In a finite-basis linear variational calculation, if we simultaneously compute the value of I_n for each state, we observe a general feature. While a true plot of I_n vs n shows the trend depicted in Figs. 1 and 2, the upper states in finite-basis calculations will be more in errors and hence the presumed logarithmic rise of I_n with n will not be found. Instead, the values will suddenly drop down after rising gradually for the first few excited states. This feature is nicely seen in two pilot calculations with mixed oscillators of the type x^2+x^{2M}. Accurate energies are available for such systems [33]. For $M=3$, we take $K=10$ and for $M=4$, we employ just six basis functions. Still, the general feature is not lost. Relevant computed data are plotted in Fig. 5. The expected variation, had all the states been correctly constructed, is shown by analytic continuation (dashed lines). Clearly, the departure from the assumed rise signals some error in calculations. We notice here that two states are bad in six-basis calculations and three are so when $K=10$. It is natural to believe that the number of

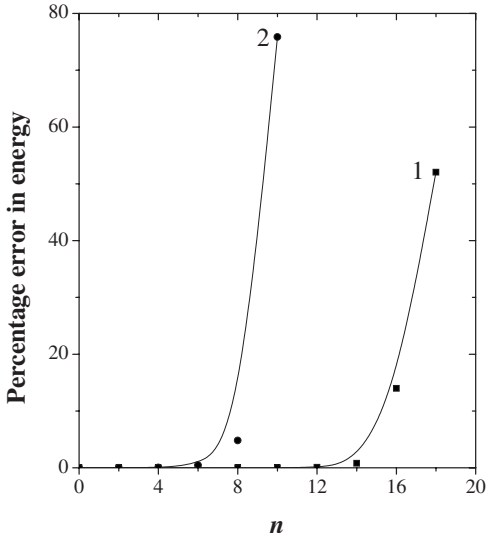

FIG. 6. Graphs showing the variations of percentage errors in energies obtained via finite-basis calculations as functions of the quantum number. Curves 1 and 2 refer to those in Fig. 5.

such states out of a given total K bases will depend both on the problem in hand and the quality of basis. But, a plot like Fig. 5 will follow in each case and it will transparently indicate the states to reject. This provides a kind of internal check. Its main appeal lies in the simplicity. For a more convincing demonstration, one may compare the energies obtained via the diagonalization procedure with the true values that are known. This stands as one of the standard measures of the goodness of the resulting states. We show in Fig. 6 the variation of percentage error with n for both the six-basis (even parity) calculation for the mixed octic oscillator (curve 2) and the ten-basis calculation for the mixed sextic one (curve 1). In the former case, the third even excited state ($n=6$) is in error by about 0.45% that rises for the next two states to 4.8% and 76%, respectively. Similarly, curve 1 shows errors of 0.09%, 0.79%, 14%, and 52%, respectively, for n values of 12, 14, 16, and 18. Thus a close look at Fig. 6 reveals that conclusions based on Fig. 5 are quite justified, though the latter does not involve any knowledge about exact energies or other properties of near-exact eigenstates. This surely counts as an advantage of the IE in practical situations. A different kind of plot in Fig. 7 involves estimates of deviation from the virial theorem, which holds for bound stationary states. We define the virial ratio (υ_r) as

$$\upsilon_r = \left\langle x\frac{dV}{dx}\right\rangle \Big/ 2\langle T\rangle \tag{41}$$

and check how far it departs from the ideal value of unity for the various states. A clear correspondence with Fig. 5 is again apparent. In case of curve 1, $\upsilon_r(n)$ shows a sudden rise from the value of 1.000 66 for $n=12$ to 1.3348 ($n=14$), 4.0023 ($n=16$), and 7.1665 ($n=18$). A very similar kind of sudden departure is observed for the last two even states of curve 2, as shown in the same figure. For more complicated problems with potentials expressed as rational functions, however, it is easier to opt for plots of the form of Fig. 5

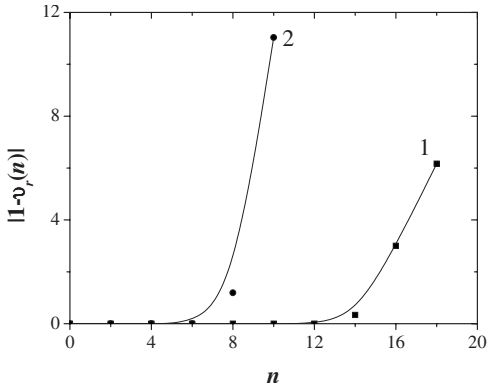

FIG. 7. Errors in virial ratios [see Eq. (41)], estimated by $|1-\upsilon_r(n)|$, as functions of the quantum number for finite-basis calculations. Curves 1 and 2 refer to those in Fig. 5.

rather than those of Fig. 7. Therefore IE offers a simpler and better alternative in checking internal consistency in such computations.

D. Stabilization method and resonances

We now turn attention to the role of IE during detection of Siegert states and estimates of real energy parts of such states by following the stabilization method with square-integrable functions. The basic idea of the method is that, unlike stationary states that are exact energy extrema, the long-lived metastable states constructed by bound functions satisfy the virtual energy extrema condition. Taking linear combinations of the *even* box states in $(-L,L)$, we prepare states by diagonalizing the Hamiltonian matrix at fixed L values and look for their stability in energies with respect to variations in L [27]. In practical terms, we select that state as a resonant one which *minimizes* $|dE/dL|$. Stationary states, on the contrary, satisfy $|dE/dL|=0$. Figure 8 shows a typical plot from where one can get such a state. A careful analysis of the figure shows that $|dE_0/dL|$ is minimum at about $L=3.501$, and the value of energy at this point is 0.902 399 50. But, one may also notice that $|dI_0/dL|$ attains a minimum here as well at a somewhat lower $L=3.35$ where the energy is 0.904 695,

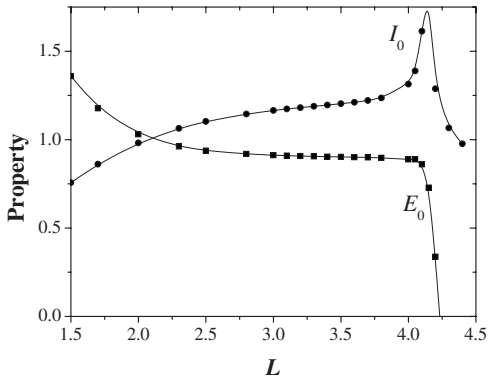

FIG. 8. Profiles of energy and information entropy during detection of a Siegert state of the anharmonic oscillator with the potential $x^2-0.1x^4$. The typical variation is against a nonlinear parameter L that forms the basis of the stabilization method.

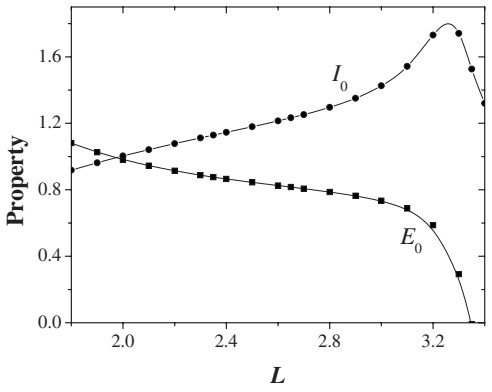

FIG. 9. The same profiles as in Fig. 8, but now for a state with a shorter lifetime, defined by the potential $x^2-0.2x^4$.

somewhat higher than what the stabilization method offers. Further, while the energy remains virtually stationary over a larger region of L, the IE covers a smaller one. This region, in both cases, reduces considerably as the lifetime shortens. Figure 9 reveals it quite clearly. Here, we observe that $|dE_0/dL|$ is minimum at about $L=2.6295$ with energy 0.820 025. But, $|dI_0/dL|$ is minimum here again at a lower L value of 2.35 at which the energy is 0.876 24. We may compare such situations with a true bound stationary-state calculation shown in Fig. 10. For the ground state, energy has a real minimum, though quite broad in our chosen scale. The IE, on the contrary, increases initially, remains virtually stationary over a considerable range, but increases again slowly. This is because of the gradual decrease of the average kinetic energy with increasing delocalization. When contrasted with the behavior in the case of Siegert states, we notice two very remarkable features of the IE. It attains a maximum at some point beyond the minimum of $|dE_0/dL|$. Then, however, it suddenly drops to a very small value. To understand these two characteristics of the IE, we show plots of the PD vs x at four L values in Fig. 11. The first two plots show the natural single-hump PD, implying stability of the particle near the origin of the potential that is a local minimum. The subsequent rise of the IE is a result of an increased delocalization involving three regions of low potentials—two at the two extremities ($\pm L$) and one at the origin. Thus we here obtain

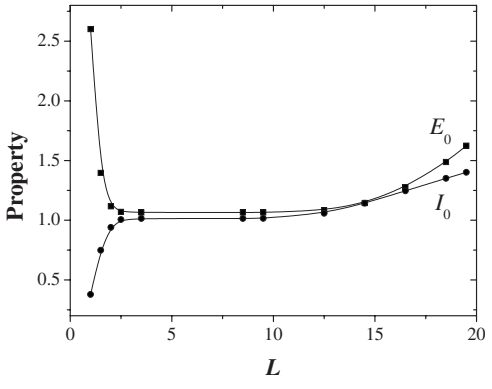

FIG. 10. Profiles of energy and information entropy for a bound state of the anharmonic oscillator with potential $x^2+0.1x^4$.

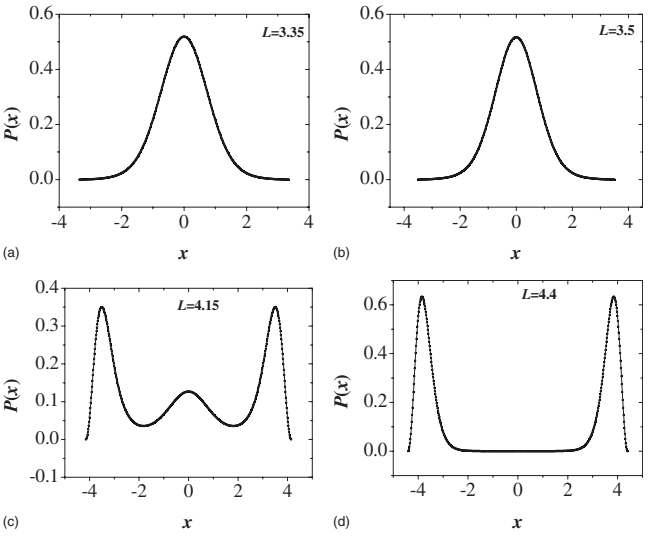

FIG. 11. Plots of the probability densities vs x during detection of a Siegert state at various values of the overall confining length L for the potential $x^2-0.1x^4$. (a) The L value around which the IE becomes almost stationary. (b) The L value around which the energy becomes almost stationary. (c) The L value around which the IE attains its maximum. (d) The behavior of the PD at some point beyond the maximum of the IE, and far beyond the point of quasistationarity of energy.

a triple-hump PD. A further increase of L considers only the extremities as the two primary low-potential regions. Therefore the PD gets concentrated only near the boundaries. This yields a double-hump PD, each hump with a narrow width, reducing the IE considerably. Any additional stretching of L only sharpens this double-hump PD and the IE goes on decreasing more.

Having understood the reasons behind the nature of variation of the IE with L, we notice that the stabilization method shows three important signatures of a Siegert state in terms of IE. First, the IE shows "stabilization" as well, like the average energy. Second, beyond a resonant state, the IE gradually rises to a maximum. Third, the IE rapidly decreases just after attaining its maximum.

V. CONCLUDING REMARKS

A direct application of the MEP to pure states of quantum systems has so far remained limited to the ground state owing to the need of simultaneously satisfying quite a few extra constraints arising out of the orthogonality and uncoupled nature of the concerned excited stationary state with respect to *all* the lower-energy states. A bypass to the problem is to investigate the variation of IE as a function of the quantum number [18]. We have here extended the analysis in various ways. It has been found that there are two competing factors. There is an increasing tendency of the PD to encompass the whole available space with increasing excitation. This raised the IE. But, an opposing aspect is provided by the additional constraints mentioned above that an excited stationary state has to satisfy. An exact balance of these two factors is found

for confined systems, i.e., those that are kept within fixed boundaries. In all the other cases, a monotonic rise of IE with excitation is observed. The reason is simple. With excitation, the effective confining region increases as well, resulting in an extra rise of the IE. Keeping it in mind that a box-type potential is only a model and that practical potentials never grow abruptly to infinity at a point, the situation is quite assuring. We can say that in all practical cases, IE tends to a maximum as $n \to \infty$ in spite of infinitude of constraints. In other words, the MEP is satisfied in the Bohr limit. There exist a variety of approaches to justify this latter limit, which is a classical limit. Here, such a regime has been connected to some PD that maximizes the IE.

We observed initially a logarithmic rise of the IE with n. Later, we have found a more precise variation of the IE with the average kinetic energy of a state. The IE of a stationary state increases logarithmically with $n^2/\langle T \rangle_n$. The calculational support is encouraging too. It provides a route to couple Shannon and Fisher measures as well. Such a link possesses a nice physical appeal. It will be interesting to seek a similar relationship for *nonstationary* quantum states. Further, we demonstrated how a study of the variation of IE with quantum number can distinctly distinguish good states from bad ones in approximate calculations for bound energy eigenstates. The relevance of studying the IE in detection of Siegert states has also been noted. Three important signatures have been obtained when the stabilization method is adopted. We additionally indicated how the nature of variation would differ in stationary-state calculations. In view of the importance of the IE in atomic and molecular calculations [24,34], our observations can profitably guide in detection of atomic resonances. Finally, most of the derivations followed an SC route via the WS rule. In the absence of a more rigorous course, this is probably the best that one can choose. However, it is comforting to note that the SC outcomes are also supported later by exact or near-exact quantum mechanical results, and that too even for the low-lying energy states. Thus the chosen strategy finds an *a posteriori* justification. Here lies the final success of the present endeavor.

ACKNOWLEDGMENT

We are thankful to an anonymous referee for a few very constructive criticisms.

[1] E. T. Jaynes, Phys. Rev. **106**, 620 (1957); **108**, 171 (1957).
[2] *The Maximum Entropy Formalism*, edited by R. D. Levine and M. Tribus (MIT Press, Cambridge, MA, 1979).
[3] N. Agmon, Y. Alhassid, and R. D. Levine, J. Comput. Phys. **30**, 250 (1979); L. R. Mead and N. Papanicolaou, J. Math. Phys. **25**, 2404 (1984); C. G. Gray, in *Maximum Entropy and Bayesian Methods in Applied Statistics*, Proceedings of the Fourth Maximum Entropy Workshop, University of Calgary, edited by James H. Justice (Cambridge University Press, Cambridge, 1984), p. 194.
[4] C. M. Bender, L. R. Mead, and N. Papanicolaou, J. Math. Phys. **28**, 1016 (1987).
[5] K. Bhattacharyya, Chem. Phys. Lett. **161**, 259 (1989).
[6] *Maximum Entropy in Action*, edited by B. Buck and V. A. Macaulay (OUP, Oxford, 1991).
[7] G. La Penna, J. Chem. Phys. **119**, 8162 (2003).
[8] D. Poland, J. Chem. Phys. **112**, 6554 (2000).
[9] A. Singer, J. Chem. Phys. **121**, 3657 (2004).
[10] A. Antoniazzi, D. Fanelli, J. Barré, P-H. Chavanis, T. Dauxois, and S. Ruffo, Phys. Rev. E **75**, 011112 (2007).
[11] J. S. Dehesa, R. J. Yanez, A. I. Aptekarev, and V. Buyarov, J. Math. Phys. **39**, 3050 (1998); V. S. Buyarov, J. S. Dehesa, A. Martinez-Finkelshtein, and E. B. Saff, J. Approx. Theory **99**, 153 (1999); B. Beckermann, A. Martínez-Finkelshtein, E. A. Rakhmanov, and F. Wielonsky, J. Math. Phys. **45**, 4239 (2004).
[12] G. E. Crooks, Phys. Rev. Lett. **99**, 100602 (2007).
[13] I. Bialynicki-Birula and J. Mycielski, Commun. Math. Phys. **44**, 129 (1975); D. Deutsch, Phys. Rev. Lett. **50**, 631 (1983); M. H. Partovi, *ibid.* **50**, 1883 (1983).
[14] R. Atre, A. Kumar, N. Kumar, and P. K. Panigrahi, Phys. Rev. A **69**, 052107 (2004); E. Aydıner, C. Orta, and R. Sever, Int. J. Mod. Phys. B **22**, 231 (2008).
[15] N. Canosa, A. Plastino, and R. Rossignoli, Phys. Rev. A **40**, 519 (1989); A. R. Plastino and A. Plastino, Phys. Lett. A **181**, 446 (1993); A. R. Plastino, M. Casas, A. Plastino, and A. Puente, Phys. Rev. A **52**, 2601 (1995).
[16] K. Bandyopadhyay, K. Bhattacharyya, and A. K. Bhattacharya, Phys. Rev. A **63**, 064101 (2001).
[17] K. Bandyopadhyay, K. Bhattacharyya, and A. K. Bhattacharya, Int. J. Quantum Chem. **88**, 691 (2002).
[18] J. S. Dehesa, A. Martınez-Finkelshtein, and V. N. Sorokin, Phys. Rev. A **66**, 062109 (2002).
[19] R. Gonzalez-Ferez and J. S. Dehesa, Phys. Rev. Lett. **91**, 113001 (2003).
[20] See, e.g., S. T. Epstein, *The Variation Method in Quantum Chemistry* (Academic, New York, 1974).
[21] B. R. Frieden, Am. J. Phys. **57**, 1004 (1989); *Science from Fisher Information: A Unification*, Second Edition (Cambridge University Press, Cambridge, 2004).
[22] B. R. Frieden, A. Plastino, A. R. Plastino, and B. H. Soffer, Phys. Rev. E **60**, 48 (1999).
[23] E. Romera, P. Sánchez-Moreno, and J. S. Dehesa, Chem. Phys. Lett. **414**, 468 (2005).
[24] R. F. Nalewajski, Int. J. Quantum Chem. **108**, 2230 (2008).
[25] A. Macias and A. Riera, Phys. Rep. **90**, 299 (1982); V. I. Kekulin, V. M. Krasnopolsky, and J. Horacek, *Theory of Resonances* (Kluwer, Dordrecht, 1989).
[26] J. Killingbeck, Phys. Lett. **65A**, 180 (1978); K. Bhattacharyya, J. Phys. B **14**, 783 (1981).
[27] K. Bhattacharyya and R. K. Pathak, J. Mol. Struct.: THEOCHEM **361**, 41 (1996).
[28] See, e.g., S. Mukhopadhyay, K. Bhattacharyya, and R. K. Pathak, Int. J. Quantum Chem. **82**, 113 (2001), and references therein.

[29] S. Gradshteyn and I. M. Ryzhig, *Table of Integrals, Series and Products* (Academic, New York, 1980).

[30] H. Orland, Phys. Rev. Lett. **42**, 285 (1979); S. Mukhopadhyay and K. Bhattacharyya, Chem. Phys. Lett. **329**, 289 (2000).

[31] F. Cooper, A. Khare, and U. Sukhatme, *Supersymmetry in Quantum Mechanics* (World Scientific, Singapore, 2001).

[32] R. K. Pathak, A. K. Chandra, and K. Bhattacharyya, Phys. Rev. A **48**, 4097 (1993); Phys. Lett. A **188**, 300 (1994).

[33] K. Bandyopadhyay, K. Bhattacharyya, and A. K. Bhattacharya, Phys. Lett. A **314**, 88 (2003).

[34] K. Ch. Chatzisavvas, Ch. C. Moustakidis, and C. P. Panos, J. Chem. Phys. **123**, 174111 (2005).